Dalton Transactions

Accepted Manuscript

This is an *Accepted Manuscript*, which has been through the Royal Society of Chemistry peer review process and has been accepted for publication.

Accepted Manuscripts are published online shortly after acceptance, before technical editing, formatting and proof reading. Using this free service, authors can make their results available to the community, in citable form, before we publish the edited article. We will replace this *Accepted Manuscript* with the edited and formatted *Advance Article* as soon as it is available.

You can find more information about *Accepted Manuscripts* in the Information for Authors.

Please note that technical editing may introduce minor changes to the text and/or graphics, which may alter content. The journal's standard Terms & Conditions and the Ethical guidelines still apply. In no event shall the Royal Society of Chemistry be held responsible for any errors or omissions in this *Accepted Manuscript* or any consequences arising from the use of any information it contains.

ROYAL SOCIETY OF CHEMISTRY

www.rsc.org/dalton

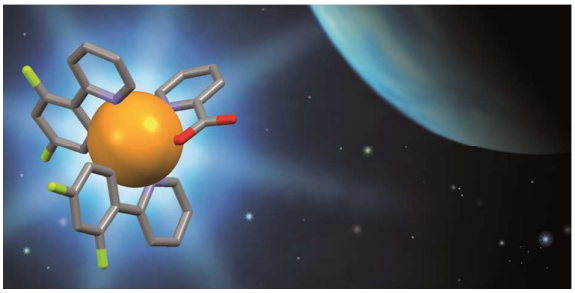

FIrpic is the most investigated bis-cyclometallated iridium complex. This *Perspective* reviews the main experimental and theoretical aspects of FIrpic as well as its use as sky-blue emitter for OLED.

Dalton Transactions Accepted Manuscript

FIrpic: archetype blue phosphorescent emitter for electroluminescence

Etienne Baranoff,[a] Basile F. E. Curchod[b]

[a] School of Chemistry, University of Birmingham, Edgbaston, B15 2TT Birmingham, UK. E-mail: e.baranoff@bham.ac.uk
[b] Department of Chemistry, Stanford University, Stanford, CA 94305-5080, USA.

Abstract.
FIrpic is the most investigated bis-cyclometallated iridium complex in particular in the context of organic light emitting diodes (OLEDs) because of its attractive sky-blue emission, high emission efficiency, and suitable energy levels. In this *Perspective* we review the synthesis, structural characterisations, and key properties of this emitter. We also survey the theoretical studies and summarize a series of selected monochromatic electroluminescent devices using FIrpic as the emitting dopant. Finally we highlight important shortcomings of FIrpic as an emitter for OLEDs. Despite the large body of work dedicated to this material, it is manifest that the understanding of photophysical and electrochemical processes are only broadly understood mainly because of the different environment in which these properties are measured, i.e., isolated molecules in solvent *vs* device.

I. Introduction

For more than a decade, cyclometallated iridium complexes have attracted enormous interest due to their unique photophysical properties and wide range of applications.[1-11] In particular since the demonstration of highly efficient organic light emitting diodes[12, 13] (OLEDs) they have been the emitters of choice for this lighting technology and thousands of complexes have been reported with electroluminescence as the key application.

Among all these different complexes, bis[2-(4,6-difluorophenyl)pyridinato-C^2,*N*](picolinato)iridium(III) (Fig. 1), commonly abbreviated **FIrpic** or Ir(diFppy)$_2$(pic), is the most used blue phosphorescent material and the most investigated bis-cyclometallated iridium complex. This success can be ascribed to a combination of straightforward synthesis, good general stability, ease of manipulation and processability, and attractive photophysical and electrochemical properties.

Dalton Transactions Accepted Manuscript

In this *Perspective* we first summarise the synthesis and characterisations followed by an account of the main properties of FIrpic. While a general understanding of FIrpic properties is available, there is still a range of values reported, in particular regarding the LUMO energy level, which can have serious consequences when selecting host and charge transporting materials for OLEDs. In the fourth part we review the theoretical studies devoted to FIrpic. It is clear that the choice of methodology has a strong impact on the results, especially concerning the degree of involvement of the picolinate ancillary ligand in the LUMO at the ground state geometry and its role in the emission property of FIrpic. In the fifth part we present selected examples of monochromatic OLEDs using FIrpic as the emitter. The choice was primarily made to highlight the improvement of device efficiency over the years: initially with EQE at about 5%, most recent devices demonstrate EQE about 30%. It shows that a full device optimisation is necessary to get the best of a given emitter. Finally we finish with a section about the shortcomings of FIrpic as an active element of electroluminescent devices.

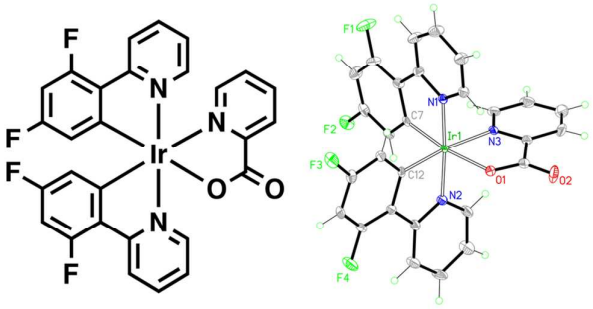

Fig. 1 Chemical structure and ORTEP drawing of FIrpic.

II. Synthesis and structure

Synthesis. One advantage of FIrpic is its ease of synthesis as it is simply obtained in three straightforward steps. First the ligand 2-(2,4-difluorophenyl)pyridine is prepared by conventional Suzuki coupling, with yields ranging from 60% to quantitative. The chloro-bridged iridium dimer is usually obtained following the method reported by Sprouse *et al.*[14] that is the reaction between $IrCl_3$ hydrate with an excess of the phenylpyridine ligand in a 3:1 v/v mixture of 2-ethoxyethanol and water under reflux for 24 hours. The reaction can also be achieved using Nonoyama's conditions[15] that is simply using 2-methoxyethanol as solvent. Recently, iridium(I) complexes such as $[Ir(COE)_2(\mu\text{-}Cl)]_2$ (COE: cyclooctene)[16] and $[Ir(COD)(\mu\text{-}Cl)]_2$ (COD: cyclooctadiene)[17]

Dalton Transactions Accepted Manuscript

have been used as starting materials with the advantage of short reaction time (1 to 3 hours). The third step consists in the coordination of the 2-picolinate ancillary ligand and can be achieved in a range of conditions, from harsh refluxing 2-ethoxyethanol with sodium carbonate as base[18] to gentle refluxing dichloromethane with tetrabutyl-ammonium hydroxide as base.[19]

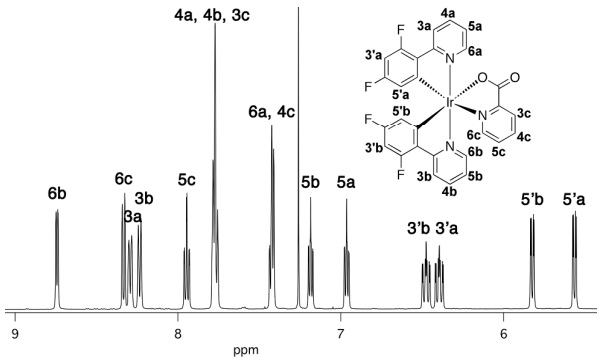

Fig. 2 ^{1}H NMR of FIrpic in $CDCl_3$.

NMR. The ^{1}H NMR spectrum of FIrpic in $CDCl_3$ is shown in Fig. 2. The 16 protons are all non-equivalent and well defined signals are observed for most of them. The effect of the pyridine ring of the picolinate ancillary ligand is seen on protons 5a and 6a, which are shielded compared to 5b and 6b because located on top of the picolinate pyridine ring. Protons 3'b and 5'b are on the contrary deshielded compared to 3'a and 5'a because they are on the side of the picolinate pyridine ring.
Solid state ^{1}H and ^{13}C NMR were reported along infra-red spectroscopy.[20]

X-ray single crystal. The X-ray single crystal structure of FIrpic has been reported[21] and the coordination geometry of the central iridium atom is a distorted octahedron with *cis*-C–C and *trans*-N–N dispositions of the two cyclometallated ligands. The Ir–O distance is 2.152(3) Å and Ir–C and Ir–N lengths are in the range of 1.993(4)–1.997(5) Å and 2.041(4)–2.138(4) Å, respectively. The structure of a co-crystal of FIrpic with one methanol molecule (forming hydrogen bond with the oxygen of the picolinate) was reported with similar geometry, Fig. 1, and slightly longer bonds (Ir–C and Ir–N lengths in the range of 2.002(3)–2.010(3) Å and 2.049(3)–2.135(3) Å, respectively).[19]

Dalton Transactions Accepted Manuscript

Table 1. Oxidation and reduction potentials of FIrpic.

E_{ox} / V	E_{red} / V	Reference	Solvent	
1.244		Ag/AgCl	MeCN	[22]
1.320		Ag/AgCl	MeCN/H_2O	[22]
1.204		Ag/AgCl	H_2O	[22]
0.89		Fc^+/Fc	DMF	[23]
0.89	–2.28 –2.60	Fc^+/Fc	MeCN	[24]
0.92	–2.29	Fc^+/Fc	MeCN	[19]
0.93	–2.28 –2.62 –2.98	Fc^+/Fc	DMF [a]	[25]
0.94	–2.32 –2.75	Fc^+/Fc	MeCN	[26]

[a] 1000 mV s^{-1}.

III. Properties

Electrochemistry and energy levels. The reported electrochemical properties of FIrpic are summarised in Table 1. In acetonitrile and DMF, the oxidation potential is quasi-reversible around 0.9 V vs Fc^+/Fc and the first reduction is also quasi-reversible around –2.3 V vs Fc^+/Fc for an electrochemical gap ΔE_{REDOX} = 3.2 eV. The reversibility of the reduction depends on the solvent and is reported irreversible in dichloromethane.[24] When scanned at 1 V s^{-1}, the three reductions for the three ligands are observed.[25] The oxidation is ascribed to oxidation of the iridium(III) metal centre to iridium(IV) whilst the first two anodic peaks are assigned to reduction of the two cyclometallated ligands and the third to the picolinate ancillary ligand.

Redox potentials obtained by cyclic voltammetry are often used to calculate the HOMO and LUMO energy levels. The energy level of ferrocenium/ferrocene is commonly quoted as 4.8 eV below the vacuum level[27] although the approach has important limitations.[28] It gives values about –5.7 eV for the HOMO and –2.5 eV for the LUMO when using the redox potentials (about –5.6 and –2.6 eV if using the onsets of the peaks[26]). The ionisation potential of FIrpic in thin film was measured at –5.91 eV[23] and –5.8 eV[29] using ultraviolet photoemission spectroscopy (UPS). A value of –6.2 eV is also reported.[30] The LUMO energy is also reported at –3.5eV,[30] –3.2 eV,[31, 32] –3.1 eV,[33] –3.0 eV,[34] –2.9 eV (in table, –2.7 in text),[29] and –2.54 eV,[35] often without much details on the methodology used to obtain the value. It is well possible that the deeper LUMO energies correspond to optical LUMOs ($E_{opt\text{-}LUMO}$ = E_{HOMO} + $E_{0\text{-}0}$, with $E_{0\text{-}0}$ = 2.7 eV).

Dalton Transactions Accepted Manuscript

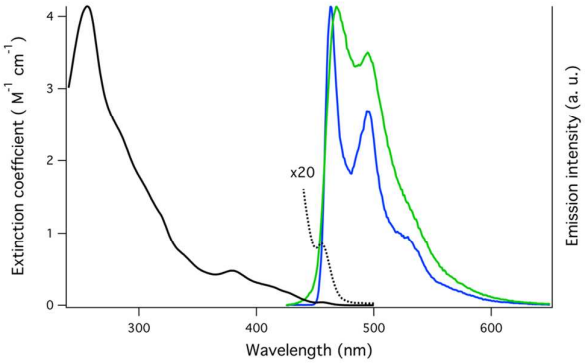

Fig. 3 Absorption (black), emission at RT (green), and emission at 77K (blue) of **FIrpic** in DCM.[19]

UV-visible absorption and emission. The UV−visible electronic absorption spectra of FIrpic in CH_2Cl_2 solution (Fig. 3) is dominated by an intense absorption band at 256 nm ($\varepsilon \approx 40 \times 10^3$ M^{-1} cm^{-1}) assigned to ligand centred (LC) $^1(\pi-\pi^*)$ transitions on the cyclometallated ligand. The weaker ($\varepsilon < 5 \times 10^3$ M^{-1} cm^{-1}) bands at lower energies (350−440 nm) have charge-transfer (CT) character related to electronic transitions from the metal centre to the cyclometallated ligands (MLCT). Finally the extremely weak peak at 455 nm is attributed to direct population of the emitting triplet state.[19, 36] A weak bathochromic shift is observed when the polarity of the solvent decreases.[19]

The room temperature emission spectrum in dichloromethane exhibits a maximum at 468 nm with a vibronic progression at 495 nm and at 535 nm (shoulder), Fig. 3. The spectrum is not sensitive to the solvent polarity.[19, 36, 37] The emission of the complex is similar in shape to the emission of diFppyH$^+$, the protonated diFppy ligand, with emission maximum at 445 nm.[19]

The photoluminescence quantum yield in dilute solution is high. Initially reported as about 60%[19, 26, 38-40] it was revaluated >80% using an integrating sphere.[37, 41, 42] The reported lifetimes of excited state in dichloromethane are 1.4,[43] 1.7,[19, 42] and 1.9 μs.[37] Assuming unitary intersystem crossing efficiency, this gives radiative constant k_R ~ 5 x 10^5 s^{-1} and k_{NR} ~10^5 s^{-1}.

At 77K in frozen dichloromethane, the emission spectrum displays intense and highly resolved bands with only a small hypsochromic shift of 5 nm, Fig. 3, and the lifetime of excited state is measured at 2.24 μs.[19]

These results and other studies point to an emitting state with mixed LC-MLCT character.[37, 44, 45]

Dalton Transactions Accepted Manuscript

Of interest for solid-state lighting applications are the luminescent properties of FIrpic in solid state, in particular when diluted in an organic host. The key property of the organic host for efficient photoluminescence is its triplet state energy: high triplet state will ensure that the excitons are transferred to and then confined on the emitter, while a low energy triplet state will act as an energy acceptor for the excited FIrpic.[32] Tanaka *et al.* have studied the temperature dependence of the phosphorescence intensity of Host:3wt% FIrpic where Host is CBP (T_1 = 2.55 eV) and CDBP (T_1 = 2.79 eV).[46] In CBP host, three different regimes were identified. Below 40 K the exothermic energy transfer from FIrpic to CBP dominates resulting in low FIrpic photoluminescence efficiency. Between 40 and 150 K, the temperature is sufficient to promote endothermic transfer from CBP to FIrpic, which increases FIrpic phosphorescence efficiency (maximum intensity at 150 K). At higher temperature, non-radiative deactivation of the CBP triplet states results in a gradual decrease of FIrpic luminescence. With CDBP as the host the temperature has no effect (up to 300 K) on the photoluminescence intensity because of the higher triplet state of the host, which confines the exciton on FIrpic. Additional temperature studies can be found in references [41] and [43].

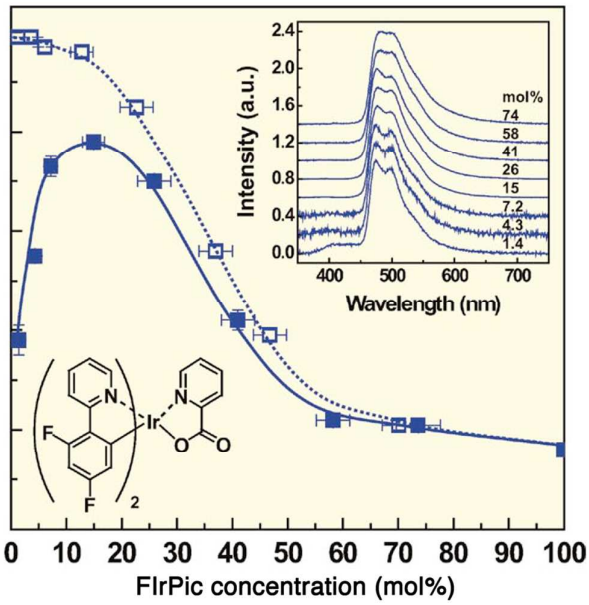

Fig. 4 PL quantum efficiency η_{PL} vs dopant concentration in FIrpic:CBP (■) and FIrpic:mCP (□). Insets show PL spectra of FIrpic:CBP measured at each dopant concentration (increasing going up on y axis): 1.4–74 mol%. Reproduced with permission from AIP (Copyright 2005).

Dalton Transactions Accepted Manuscript

The dopant concentration also plays an important role for high luminescence efficiency of films. Kawamura *et al.* have studied the concentration dependence of the phosphorescence of Host:Xmol% FIrpic where Host is CBP and mCP (T_1 = 2.91 eV) and X varied from 1.2 to 100 (Fig. 4).[47] When CBP, which has a lower triplet state than FIrpic, is used as the host, the photoluminescence efficiency initially increases from 38±4% at 1.4 mol% to 78±1% at 15 mol% (Fig. 4) because of the back energy transfer from FIrpic to CBP.[38] With mCP as the host, the photoluminescence efficiency is 99±1% at 1.4 mol% because of the good confinement of the triplet exciton on FIrpic. As the concentration of FIrpic increases, the photoluminescence efficiency decreases down to 16±1% for the neat film. This concentration quenching has been found to be dependent on $1/R^6$, with R the distance between dopant molecules.[48] This dependency on R points to Förster energy transfer as a mechanism of deactivation. Because the dipole-dipole interactions will be between triplet states with low oscillator strength, the Förster radius R_0 was found 1.4±0.1 nm for FIrpic, much smaller than for conventional fluorescent dyes.

Charge mobility. The electron and hole mobilities of FIrpic have been studied by time-of-flight (TOF) measurements in neat film[49] and doped into CBP films.[49] In neat films, FIrpic exhibits both electron and holes mobilities on the order 10^{-7}-10^{-6} cm^2 V^{-1} s^{-1}. When doped in CBP films, the hole mobility is much higher but decreases with increasing FIrpic concentration, while electrons are found not to be mobile. The authors also calculated the diffusion lengths of the FIrpic exciton in 3.5% and 7.0% FIrpic-doped CBP thin films, which are 250 and 310 nm, respectively.

IV. Theoretical studies on FIrpic

Density Functional Theory[50, 51] (DFT) and linear-response time-dependent density functional theory[52-55] (LR-TDDFT, also abbreviated TDDFT or TD-DFT, allowing calculations of electronic excited states) with hybrid exchange-correlation functionals are by far the most applied methods to study iridium emitters.[56, 57] The notoriety of these methods is due to their capability of treating efficiently and rather accurately these medium- to large-size molecules (see Ref. [58] for a review of these two methods in the OLED context). For detailed and pedagogical discussions on LR-TDDFT and its limitations, the interested reader is referred to Refs. [39, 43, 44] We propose in the following a brief survey of selected calculations done on the FIrpic emitter, followed by a general discussion on different computed properties.

Dalton Transactions Accepted Manuscript

One of the first theoretical study of FIrpic has been proposed by Kim *et al.* in 2006.[59] A ground-state optimised geometry was obtained with DFT/B3LYP[60, 61] and compares well with FIrpic X-ray structure. The Kohn-Sham (KS) frontier orbitals were presented, together with the transition energies at the ground state geometry obtained with LR-TDDFT at a similar level of theory.

In 2008, Zhang, Ma, *et al.* compared FIrpic and FIracac in a purely computational article.[62] Geometries were optimised for both the (singlet) ground state and the first triplet state with LR-TDDFT/PBE0[63] and CIS, respectively. Compared to the ground-state geometry, only a weak elongation of the Ir-C and Ir-N bonds was observed for the triplet-state structure. A first approximation to the emission energy was obtained by calculating triplet-to-singlet energy differences with LR-TDDFT at the triplet-state optimised geometry. Based on these calculations, the character of FIrpic emission was assigned to a metal-to-ligand/intraligand charge transfer.

Koseki *et al.* proposed an intensive discussion on FIrpic-like molecules using density- and wavefunction-based methods and including the effect of spin-orbit coupling,[64] rationalizing the different stability and properties of [Ir(diFppy)$_2$(pic)] isomers.

In a mixed experimental/theoretical work, Tsai *et al.* studied FIrpic with Raman and Infrared spectroscopy.[65] As calculated molecular geometries for the ground state are usually compared with X-Ray structures, the good agreement between theory and experiment for band positions and spectra intensity provides an additional validation of DFT accuracy for treating FIrpic.

In another study,[19] the absorption spectra of FIrpic has been theoretically studied using LR-TDDFT/M06[66] and incorporating spin-orbit coupling effects, confirming that the low-energy tail of the absorption spectra is due to relativistic effects. FIrpic triplet geometry was optimised with DFT/M05-2X[67] and the triplet-to-singlet transition exhibits a LC-MLCT character on a diFppy ligand, as further confirmed by LR-TDDFT and in agreement with Ref. [62].

Recently, Brédas and coworkers explored in a detailed article how the substituents on the ancillary ligands acetyl acetonate, picolinate, and pyridylpyrazolate affect the emission properties for a large family of iridium complexes, comprising FIrpic.[68] For the latter, theory, (LR-TDDFT/B3LYP) confirmed that the ancillary ligand does not participate directly to the emission process and therefore only weak indirect effects can be expected upon picolinate substitution. In addition, DFT/B3LYP proposes that the meridional isomer of FIrpic, with the two N atoms of the diFppy ligands being *trans* to each other, is the most stable one (for additional comments on FIrpic isomers, see the section on Stability).

Dalton Transactions Accepted Manuscript

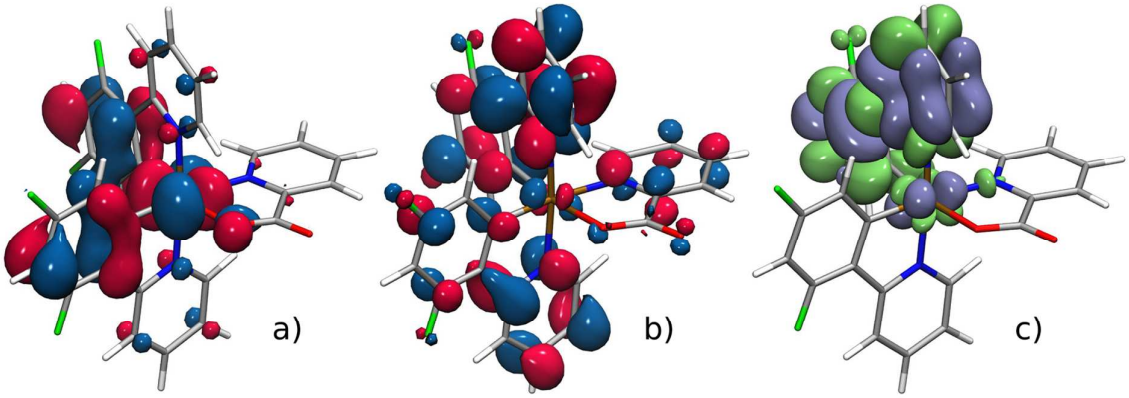

Fig. 5 FIrpic Kohn-Sham highest occupied (a) and lowest unoccupied (b) orbitals (DFT/M06). c) Electronic density difference plot for the first triplet state of FIrpic (LR-TDDFT/M05-2X), where the hole is showed in blue and the electron in green.

An interesting common feature of these different studies is the analysis of the frontier KS orbitals (as a *caveat*, it is first important to mention that in DFT, the HOMO-LUMO energy gap is closely related to the optical gap and not to a fundamental band gap like in Hartree-Fock theory[69, 70]). The KS-HOMO is mostly localized on the iridium and the phenyl part of the diFppy ligand at the ground-state optimised geometry, while the KS-LUMO contains a certain contribution from the picolinate (Fig. 5a and b).[19, 59, 62, 71-73]

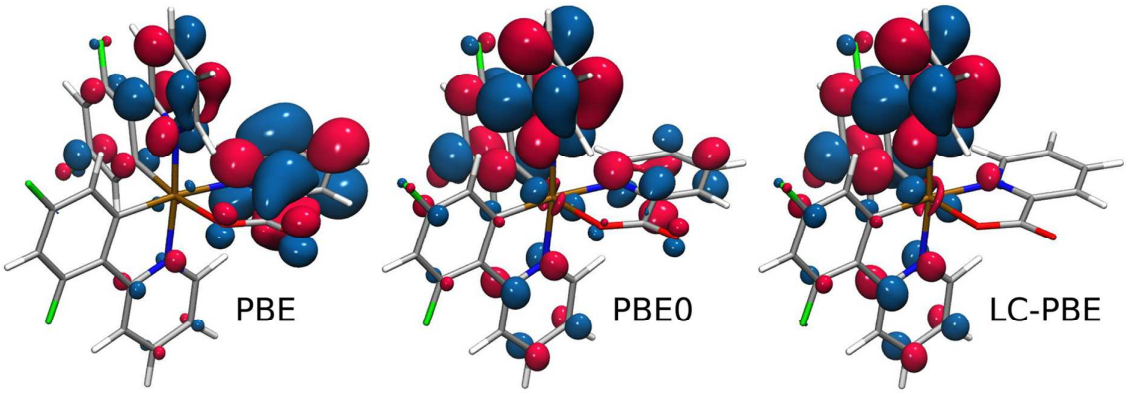

Fig. 6 FIrpic Kohn-Sham lowest unoccupied orbitals (DFT/M06 geometry) as computed with PBE (0% of exact exchange), PBE0 (25% of exact exchange) and LC-PBE[74] (variable amount of exact exchange) with the same basis set (SBKJC/VDZ and 6-311G*).

Dalton Transactions Accepted Manuscript

However, LR-TDDFT predicts that the first triplet state computed at the ground-state optimised geometry does not have a dominant HOMO–>LUMO contribution but a HOMO–>LUMO+1.[62] The electronic configuration of the first triplet state is therefore characterised by an electron being transferred from a mostly metal d orbital to a π^* orbital principally situated on the diFppy ligands, and not on the picolinate, as could have been postulated from a simple analysis of the frontier orbitals. These results show the potential limitation of a purely orbital-based analysis of electronic states at the ground-state geometry. The KS HOMO-LUMO gap is only an approximation to the true optical gap and by including the response of the Coulomb and exchange-correlation potential due to the changes in the electronic density, LR-TDDFT shows that electronic states with other occupied-to-virtual orbital contributions can actually be lower in energy than the one described by a HOMO–>LUMO transition. It is finally interesting to note that the picolinate contribution to the FIrpic LUMO is likely to depend on the computational protocol, such as the basis set, inclusion of solvent, or the exchange-correlation functional in DFT (Fig. 6).

DFT, when using hybrid exchange-correlation functionals such as PBE0 or B3LYP, predicts a ground-state geometry for FIrpic in reasonable agreement with X-ray structures. Computed Ir-C_{ppy} (Ir-N_{ppy}) bond lengths range from 1.995 to 2.025 Å (2.030 to 2.074 Å), while the bond length between Ir and the coordinating atoms of the picolinate ligand are usually found at slightly larger values, with 2.134 to 2.206 Å for Ir-N_{pic} and 2.144 to 2.180 Å for Ir-O_{pic}.

Upon relaxation of the molecular geometry in the lowest triplet state, different studies report an MLCT-LC character for the T_1–>S_0 transition with orbital contributions from the diFppy ligands and not from the picolinate (Fig. 5c).[19, 59, 62, 68]

At the triplet optimised geometry, the energy gap computed between the lowest triplet and the singlet ground state varies moderately depending on the method used (we note here that some differences are likely to occur due to differences in basis set and the inclusion of an implicit solvent). LR-TDDFT gives vertical emission energies at 2.37 eV (PBE0 based on a CIS triplet geometry[62]), 2.28 eV (B3LYP based on a B3LYP triplet geometry[68]), 2.50 eV (B3LYP based on a CIS triplet geometry[71]), and 2.36 eV (M05-2X based on an M05-2X triplet geometry, with implicit solvent[19]). For the latter example the Δ-SCF energy gap (two DFT calculations, one for the triplet state and one of the singlet ground state) gives a singlet/triplet vertical gap of 2.66 eV with the functional M05-2X. These calculations of singlet/triplet energy gaps miss contributions from spin-orbit coupling and comparison with experiment would in addition necessitate the inclusion of vibronic effects. While scalar relativistic effects, affecting the geometry of iridium complexes, are usually incorporated by means of relativistic all-electron approaches or effective-core potentials (see Refs. [58, 75] and

Dalton Transactions Accepted Manuscript

Refs. [56, 58, 76], respectively, for different examples of iridium complexes geometries), electronic structure calculations of iridium complexes including spin-orbit coupling are less common.[17, 19, 64, 76-83] For example, a wavefunction-based method including spin-orbit coupling (MCSCF+SOCI, no solvent effects, DFT-optimised triplet geometry) predicts excitation energies for the three sublevels of T_1 at 2.72, 2.73, and 2.76 eV,[64] in excellent agreement with experiment.[36, 37]

It is important to mention that calculations are usually performed on an isolated molecule, possibly including an implicit solvent, in a *static* (single point calculation) picture. Such models are of great quality to reproduce UV/Vis spectra for example, but a reasonable photophysical and photochemical characterization of FIrpic would necessitate the use of excited-state *dynamics*. In addition, it is worth keeping in mind that processes taking place in a running device are rather different than those arising after photoexcitation (see for example Ref. [84]) and their theoretical description is by far non-trivial.

V. Organic Light-Emitting Diodes

Due to its suitable properties and ease of preparation and processing, FIrpic has been widely used as sky-blue emitter for both monochromatic and white OLEDs. Here we will briefly present a few selected examples of devices to show how the performances of monochromatic FIrpic-based OLEDs have improved over the years. FIrpic was also used as sky-blue emitter for white OLEDs, which we won't discuss in this review, see for example references [85] and [86], as well as solution-processed devices, for example see ref. [94-96], because of the much lower performances.

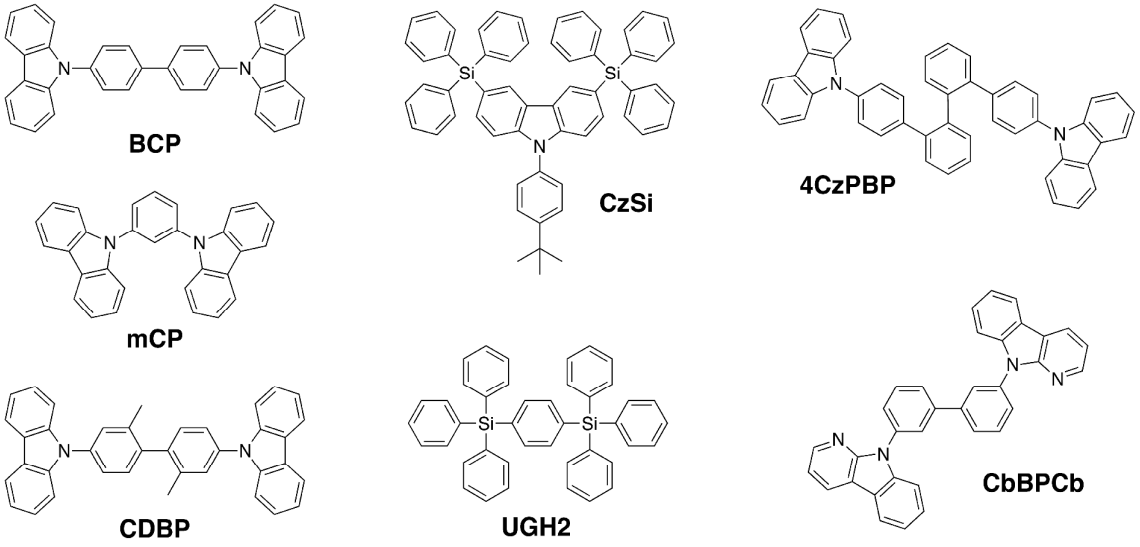

Fig. 7 Chemical structure of the host materials used in selected FIrpic-based OLEDs.

Dalton Transactions Accepted Manuscript

The first reported device based on FIrpic as the emitter used 4,4'-*N,N'*-dicarbazole-biphenyl (CBP, Fig. 7) as the host material.[38] The full device structure was: ITO as the anode, copper phthalocyanine (CuPC, 10 nm) as hole injection layer (HIL), 4,4'-bis[*N*-(1-naphthyl)-*N*-phenyl-amino]biphenyl (α-NPD, 30 nm) as hole transport layer (HTL), CBP doped with 6 wt% FIrpic as emissive layer (EML, 30 nm), 4-biphenyloxolato aluminium(III)bis(2-methyl-8-quinolinato)4-phenylphenolate (BAlq, 30 nm) as electron transport layer (ETL), and LiF (1 nm)/aluminium (100 nm) as the cathode.

The electroluminescence (EL) spectrum of the device is very similar to photoluminescence spectrum. The maximum emission is at 475 nm with subpeaks at 495 and 540 nm. The corresponding CIE coordinates are (*x*=0.16, *y*=0.29).

The device achieved a maximum external quantum electroluminescent (EL) efficiency η_{ext} of (5.7±0.3)% at a current density J = 0.5 mA cm^{-2} and a maximum luminous power efficiency η_p of (6.3±0.3) lm W^{-1} at J = 0.1 mA cm^{-2}. Due to triplet-triplet annihilation η_{ext} decreased with increasing the current density, and at J = 100 mA cm^{-2} a maximum luminance of 6,400 cd m^{-2} was obtained with η_{ext} = 3.0%.

In this case CBP has a triplet energy at 2.56 eV, lower than the triplet energy of FIrpic at 2.62 eV, therefore the favourable direction of the energy transfer is from FIrpic to CBP and the excitons are poorly confined. When a host with higher triplet energy than FIrpic was used, improved device performances were obtained.[87] Using N,N'-dicarbazolyl-3,5-benzene (mCP, triplet energy 2.9 eV) in place of CBP, keeping the overall device architecture identical, boosted η_{ext} to (7.5±0.8)% and η_p to (8.9±0.9) lm W^{-1} at low current density. At J = 100 mA cm^{-2} the performances are also higher than with CBP, reaching 9,500 cd m^{-2} with η_{ext} = 4.6%.

Further increasing the triplet energy of the host to 3.0 eV with 4,4'–bis(9-carbazolyl)-2,2'-dimethyl-biphenyl (CDBP) resulted in a device with over 10% external quantum efficiency.[88] The device architecture is ITO/PEDOT:PSS (40 nm)/α-NPD (30 nm)/host + 3 wt% FIrpic (40 nm)/BAlq (30 nm)/LiF (1 nm)/Al (150 nm). It is similar to the architecture of previous devices and the use of PEDOT:PSS instead of CuPC cannot explain the jump in performance. Indeed a device with CBP as the host was prepared and maximum η_{ext} = 5.1% was obtained with PEDOT:PSS (to be compared to η_{ext} = 5.7% with CuPC, see above). The EL spectrum peaks at 472 nm and at J = 0.1 mA cm^{-2}, the maximum η_{ext} is 10.4% with η_p of 10.5 lm W^{-1} and current efficiency of 20.4 cd A^{-1}. At J = 100 mA cm^{-2}, η_{ext} is still ~6% and at a maximum voltage of 15.5 V the device reached 20,000 cd m^{-2}.

Dalton Transactions Accepted Manuscript

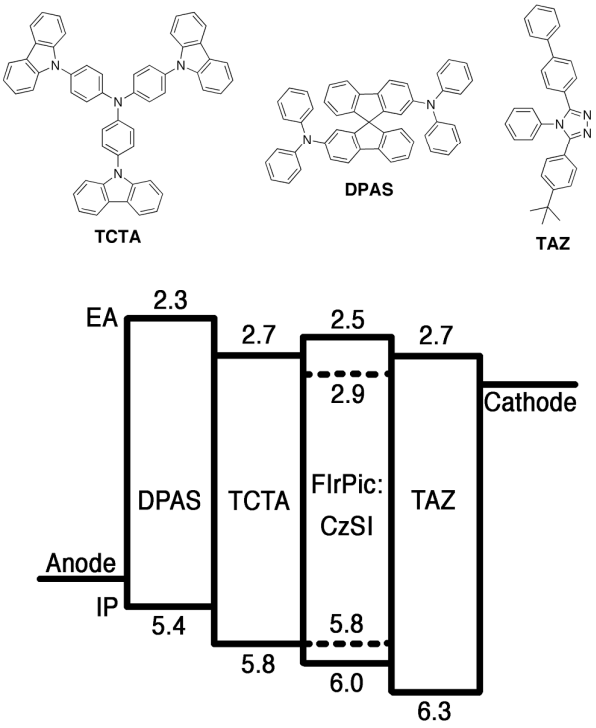

Fig. 8 Chemical structures and energy levels of related compounds in thin films.

Improved external efficiency >15% has been obtained with a device having two HTL with a stepwise increase of ionisation potentials (IPs) in order to match the IP of the host of the emissive layer.[89] The device structure used, Fig. 8 with energy levels of the compounds, is ITO/PEDOT:PSS (30 nm)/DPAS or α-NPD (17.5 nm)/TCTA (2.5 nm)/CzSi doped with 8 wt% FIrpic (25 nm)/TAZ (50 nm)/LiF (0.5 nm)/Al (150 nm), where the conducting polymer poly(ethylene dioxythiophene)/poly(styrene sulfonate) (PEDOT:PSS) is used as the hole-injection layer. The host 9-(4-tertbutylphenyl)-3,6-bis(triphenylsilyl)-9H-carbazole (CzSi) possesses a high triplet energy of 3.02 eV with an ionisation potential of 6.0 eV (from UV photoemission spectroscopy measurements). With two hole transporting layers, DPSA/TCTA or α-NPD/TCTA, maximum η_{ext} = 15.7% and η_p = 26.7 lm W^{-1} with current efficiency of 30.6 cd A^{-1} are obtained at very low current density (0.001 mA cm^{-2}) and maximum luminance of 59,000 cd m^{-2} is obtained at 14.5 V. At practical brightness of 100 cd m^{-2}, obtained at J = 0.36 mA cm^{-2}, η_{ext} is still above 12% and η_p ~16 lm W^{-1} with current efficiency of 24 cd A^{-1}. Using only one hole transporting layer of α-NPD, DPAS, or TCTA increases the operating voltage in turn decreasing the efficiency of the device.

Dalton Transactions Accepted Manuscript

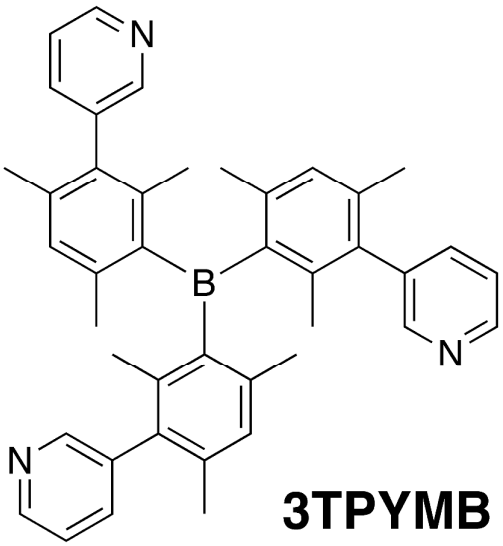

Fig. 9 Molecular structure of electron transport **3TPYMB**.

In addition to optimisation of the hole transport side of the device, utilisation of electron transport materials with high charge mobility is a successful strategy to improve the performances of the device. In 2007, Kido and co-workers reported tris[3-(3-pyridyl)-mesityl]borane (3TPYMB, Fig. 9) as an electron transport material with high electron mobility of 10^{-5} cm^2 V^{-1} s^{-1}, that is about one order of magnitude higher than tris(8-quinolinolato)aluminum (Alq_3).[90] In combination with a good hole transport material, bis[4-(*p*,*p'*-ditolylamino)-phenyl]diphenylsilane (DTASI), they reported the first FIrpic-based device with η_{ext} over 20%.[91] The structure of the device was ITO/TPDPES: 10wt% TBPAH (20 nm)/DTASI (20 nm)/4CZPBP: 13wt% FIrpic (10 nm)/3TPYMB (50 nm)/LiF (0.5 nm)/Al (100 nm) where poly(arylene-ether-sulfone)-containing tetraphenylbenzidine (TPDPES) doped with 10 wt% tris(4-bromophenyl)aminium hexachloroantimonate (TBPAH) acts as the hole injection layer and 2,2'-bis(4-carbazolylphenyl)-1,10-biphenyl (4CZPBP, Fig. 7) is a host material with triplet energy similar to FIrpic. Importantly, both 3TPYMB and DTASI have triplet energy about 3 eV, which is higher than FIrpic, allowing for good confinement of exciton within the emissive layer. At practical luminance of 100 cd m^{-2}, η_{ext} = 21% and η_p = 39 lm W^{-1} with current efficiency about 40 cd A^{-1} were obtained.

So and co-workers have compared 3TPYMB with BCP as ETL in a device using 1,4-bis-triphenylsilylbenzene (UGH2, Fig. 7) doped with 10wt% FIrpic as the emissive layer.[92] The 3TPYMB device reached maximum η_{ext} = 23% and η_p = 31.6 lm W^{-1} with current efficiency of 49 cd A^{-1}, while the BCP device showed η_{ext} = 15.3% with current efficiency about 30 cd A^{-1}.

Dalton Transactions Accepted Manuscript

Recently, devices with η_{ext} above 30% have been reported.[93] The device architecture was as follow: ITO (50 nm)/PEDOT:PSS (60 nm)/TAPC (20 nm)/mCP (10 nm)/ CbBPCb: 10wt% FIrpic (25 nm)/TSPO1 (35 nm)/LiF (1 nm)/Al (200 nm) where CbBPCb is 3,3'-bis(9*H*-pyrido[2,3-*b*]indol-9-yl)-1,1'-biphenyl, Fig. 7, a host with triplet energy similar to FIrpic, deep HOMO energy level at –6.25 eV (obtained from cyclic voltammetry measurement), and hole/electron mobility of 6.33×10^{-7} and 3.83×10^{-6} $cm^2\ V^{-1}\ s^{-1}$, respectively. The maximum η_{ext} was 30.1% and η_p = 50.6 lm W^{-1} with current efficiency of 53.6 cd A^{-1}. The external quantum efficiency remained high at 100 cd m^{-2}, 30.0%, and even at 1,000 cd m^{-2} with value of 28.4%. These excellent values were attributed to (i) a good overlap of the emission of CbPBCb with the absorption band of FIrpic favourable for efficient energy transfer to the emitter, (ii) balanced charge density in the emitting layer, (iii) good confinement of the triplet excitons in the emitting layer due to higher triplet energy of mCP and TSPO1, and (iv) the thin layer of ITO, only 50 nm, with high transmittance in the blue wavelength range.

VI. Issues with FIrpic as a phosphorescent emitter for OLEDs

As seen in the previous section, FIrpic-based devices can achieve very high efficiency. However, FIrpic has specific issues that preclude FIrpic from being a fully satisfying phosphorescent emitter for OLEDs.

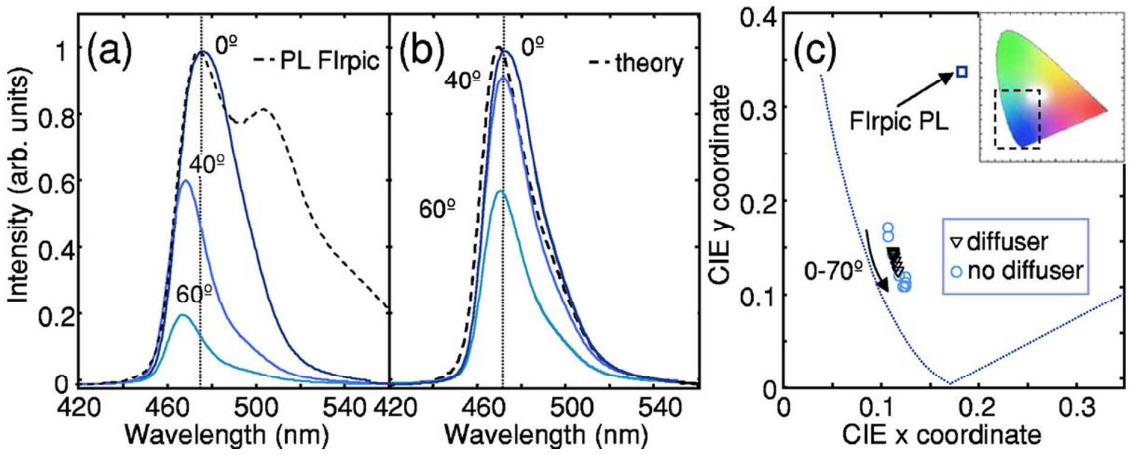

Fig. 10 Electroluminescent spectra of the strong microcavity FIrpic OLED as a function of angle from the surface normal (a) without and (b) with the holographic diffuser. (c) The CIE colour coordinates of the OLEDs and FIrpic photoluminescence spectrum. Reproduced with permission from AIP (Copyright 2007).

Colour purity. FIrpic maximum emission is at about 472 nm but the spectrum covers wavelengths from about 450 nm to over 600 nm due to vibrational levels.

Dalton Transactions Accepted Manuscript

Consequently the CIE colour point is in the bluish-green region with (x,y) coordinates about (0.18, 0.33) with some minor variations among the devices. This colour point is not suitable for display applications, which require much deeper blue. Mulder *et al.* have demonstrated saturated blue phosphorescence from a FIrpic-based OLEDs using a strong microcavity combined with a scattering layer.[97] The organic layers of the multilayer OLED are sandwiched between two reflective electrodes (silver anode and aluminium anode) and the resonant wavelength of the microcavity was set at about 450 nm. Only the highest energy part of FIrpic emission has a favourable outcoupling efficiency and the lowest energy part of the emission is dissipated within the device. As a result the EL profile of the device is much thinner (Fig. 10a) and the colour point of the device is significantly moved to deeper blue (Fig. 10c) however with a slight colour shift with the viewing angle. A holographic diffuser was added as a transparent scattering layer on the top of the glass. The resulting colour coordinates are (x,y) = (0.116, 0.136) with minimal angular colour shift and a nearly ideal Lambertian angular emission profile (Fig. 10b and 10c).

Roll off efficiency. As roll off efficiency is a general issue with phosphorescent emitter, that is not specific to FIrpic, we will only briefly mention it here. At high current density, when the density of excitons is high in the emissive layer, the efficiency of the device decreases rapidly due to triplet–triplet annihilation (TTA) and triplet–polaron annihilation (TPA). Approaches to limit this issue consist in optimisation of the carrier recombination to decrease charge accumulation and enlarging the recombination-emission zone to decrease the density of excitons and reduce annihilation processes. In practice, blending of hole and electron transport hosts[98] and using two emissive layers with separated hole and electron transport hosts[99] have been used in devices with FIrpic as the emitter.

Stability. The stability of blue phosphorescent OLEDs is still an on going issue. In addition to problems common to all OLEDs, blue phosphors present additional challenges,[100] especially thermally accessible non-radiative metal centred states.[101,102] FIrpic is further disadvantaged because of chemical complication arising from its chemical structure.

In 2009, Sivasubramaniam *et al.* have reported an in depth study of the stability of FIrpic in monochromatic FIrpic-based OLEDs.[103] First they analysed FIrpic samples before and after sublimation by liquid chromatography coupled with electron spray ionisation mass spectrometry (LC-ESI-MS). The unprocessed sample contains small amount of an isomer of FIrpic (Isomer I), a complex without picolinate (FIrpic–Pic), and a complex with only 3 fluorine atoms (FIrpic–1F). The sublimed samples contain

Dalton Transactions Accepted Manuscript

only a small amount of FIrpic–1F, demonstrating improved purity and pointing to the need of multiple sublimations to obtain pure samples.

Fig. 11 FIrpic (**Isomer II**) and possible chemical structures for isomers observed in aged devices.

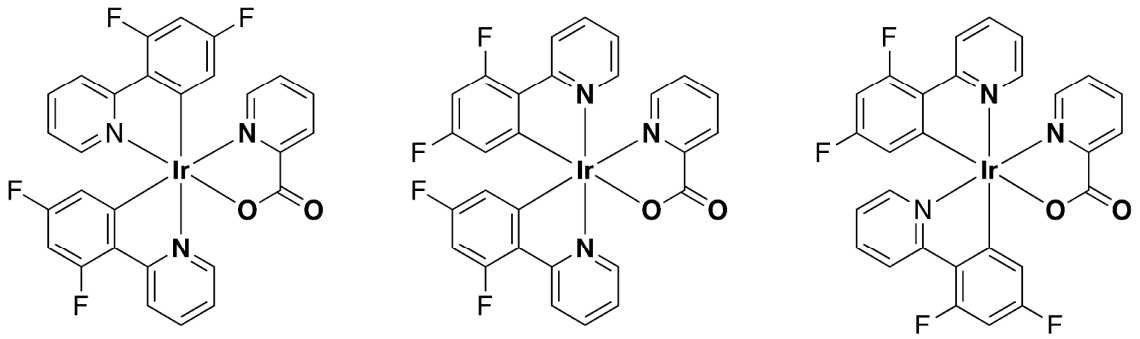

Possible **Isomer I** **Isomer II** Possible **Isomer III**

Then analyses were performed on devices. Interestingly, the pristine devices contain another isomer of FIrpic (Isomer III) along FIrpic–1F, showing that sublimation for purification and for device fabrication can lead to a different outcome. Based on the similarity of the chromatograms, **Isomer III** could be attributed to the structure shown in Fig. 11, that is a complex with the pyridines of the main ligand in cis-geometry with one pyridine in trans to the pyridine of picolinate.[104] By deduction, **Isomer I** could have the structure given in Fig. 11. In aged devices, in addition to compounds found in pristine devices, **Isomer I** is also observed with FIrpic–Pic and additional amount of FIrpic–1F. Theoretical calculations of FIrpic isomers[64, 68] indicate that **Isomer 2** is the lowest energy isomer, followed closely by **Isomer 3** (~1 kcal/mol higher in energy). **Isomer 1** is the less stable of the three isomers and lies at ~5 kcal/mol from **Isomer 2**. Similar trends for the stability of the three isomers are observed for the triplet-optimized geometries.[68] The thermally induced isomerisation may participate to the defluorination process. Indeed defluorination has been reported for a difluoro-containing complex during thermally induced *mer* to *fac* isomerisation while the *fac* complex is thermally stable.[105]

In another study on the same devices, Sivasubramaniam *et al.* suggested that mobile protons could be formed in the device upon degradation of hole transporting materials.[106] These protons can be responsible for the cleavage of the picolinate ligand as shown in the recent study about the effect of acids on such complex.[17] The use of acidic PEDOT:PSS is expected to lead to similar degradation over time.

These studies show that FIrpic is particularly instable in devices primarily due to its chemical structure and both fluorine and picolinate should be avoided for improved

Dalton Transactions Accepted Manuscript

stability. These degradation products have different optoelectronic properties compared to FIrpic, in particular a red shifted emission and destabilisation of the HOMO energy level is expected for FIrpic–1F, and can act as charge and exciton traps and participate to further chemical reactions leading ultimately to the failure of the device.

VII. Conclusion

FIrpic is the most investigated bis-cyclometallated iridium complex. With the large body of studies dedicated to FIrpic, a general picture of its properties emerges. When photoexcited in solution, it emits sky blue light from a mixed LC-MLCT excited state with an emission maximum about 470 nm, emission quantum yield up to 80% and lifetime of excited state in the region of 1.7 μs, which gives radiative and non-radiative rate constants about 5 x 10^{-5} s^{-1} and 10^{-5} s^{-1}, respectively. In solid state, the properties of the film are very dependent upon composition in terms of amount of FIrpic and triplet energy level of the host. In mCP (higher triplet energy than FIrpic) low doping levels result in virtually quantitative emission quantum yield. As the amount of FIrpic increases the emission intensity decreases due to self-quenching by Förster energy transfer.

In solution it shows oxidation at 0.9 V vs Fc^{+}/Fc and first reduction at –2.3 V vs Fc^{+}/Fc. Such values have been used to estimate the HOMO (–5.7 eV) and LUMO (–2.5 eV) energy levels, which are important parameters to devise an efficient OLED architecture and choose suitable materials. However properties in solution may not be directly used as an assumption for properties in solid state. UPS has been used to measure the ionisation potential of FIrpic and values ranging from –5.7 eV to –6.2 eV have been reported. Concerning the LUMO energy level, values spanning 1 eV have been reported (from –3.5 eV to about –2.5 eV), with too often too little details about the methodology employed to obtain such data. This has undoubtedly a significant impact on device optimisation and rationalisation of device performance. The worst situation is arguably when authors use their own measurements for some materials and, for other materials, rely on published data obtained with different methodologies.

FIrpic has been used as phosphorescent emitter for sky-blue OLEDs for more than a decade. During that period, external quantum efficiency improved from about 5% to 30% for most recent devices and luminous power efficiency increased also significantly form about 6 lm W^{-1} to about 50 lm W^{-1}. These progresses can be largely attributed to the development of new host and charge transporting materials, which demonstrates that a good emitter alone is not sufficient to obtain a good device. The shortcomings of FIrpic as an emitter for OLEDs are its unattractive CIE

Dalton Transactions Accepted Manuscript

colour point for display, significant roll off efficiency impacting the device architecture, and low stability due to chemical degradation in devices.

Numerous theoretical studies have focussed on FIrpic. Overall the absorption and redox properties are reasonably well reproduced and support the general understanding of this complex. The main challenge is to characterise the excited states. A simple molecular orbital analysis in the ground state would point to the direct involvement of the picolinate ancillary ligand in the first triplet excited state because of its participation to the LUMO. However LR-TDDFT predicts that the first triplet state computed at the ground-state optimised geometry has a dominant HOMO–>LUMO+1 contribution not involving the ancillary ligand. Theoretical calculations further confirm the indirect role played by the picolinate ligand in the emission.

As a final remark, most of what is known about FIrpic comes from studies in different conditions to within a device and it is important to keep in mind that processes taking place in a functioning device are rather different than those arising after photoexcitation. This leaves a lot of opportunities for additional experimental and theoretical studies focussing on FIrpic.

Acknowledgments

E.B. acknowledges the European Union (HetIridium, CIG322280) and B.F.E.C. acknowledges the Swiss National Science Foundation (fellowship P2ELP2_151927) for financial support. The authors also express their gratitude to Yanouk Cudré for providing Fig. 2.

References.

1. L. Flamigni, A. Barbieri, C. Sabatini, B. Ventura and F. Barigelletti, *Top. Curr. Chem.*, 2007, **281**, 143.
2. Y. You and S. Y. Park, *Dalton Transactions*, 2009, 1267.
3. Y. You and W. Nam, *Chemical Society reviews*, 2012, **41**, 7061.
4. S. Ladouceur and E. Zysman-Colman, *Eur. J. Inorg. Chem.*, 2013, **2013**, 2985.
5. E. Baranoff, J. H. Yum, M. Graetzel and M. K. Nazeeruddin, *Journal of Organometallic Chemistry*, 2009, **694**, 2661.
6. M. S. Lowry and S. Bernhard, *Chem. Eur. J.*, 2006, **12**, 7970.
7. Y. Chi and P. T. Chou, *Chemical Society Reviews*, 2010, **39**, 638.
8. V. Marin, E. Holder, R. Hoogenboom and U. S. Schubert, *Chemical Society Reviews*, 2007, **36**, 618.
9. C. Ulbricht, B. Beyer, C. Friebe, A. Winter and U. S. Schubert, *Adv. Mater.*, 2009, **21**, 4418.
10. Q. A. Zhao, F. Y. Li and C. H. Huang, *Chemical Society Reviews*, 2010, **39**, 3007.
11. K. K.-W. Lo and K. Y. Zhang, *RSC Advances*, 2012, **2**, 12069.
12. C. Adachi, M. A. Baldo, M. E. Thompson and S. R. Forrest, *J. Appl. Phys.*, 2001, **90**, 5048.
13. M. A. Baldo, M. E. Thompson and S. R. Forrest, *Nature*, 2000, **403**, 750.

Dalton Transactions Accepted Manuscript

14. S. Sprouse, K. A. King, P. J. Spellane and R. J. Watts, *J. Am. Chem. Soc.*, 1984, **106**, 6647.
15. M. Nonoyama, *Journal of Organometallic Chemistry*, 1975, **86**, 263.
16. M. W. Thesen, H. Krueger, S. Janietz, A. Wedel and M. Graf, *J. Polym. Sci., Part A: Polym. Chem.*, 2010, **48**, 389.
17. E. Baranoff, B. F. E. Curchod, J. Frey, R. Scopelliti, F. Kessler, I. Tavernelli, U. Rothlisberger, M. Gratzel and M. K. Nazeeruddin, *Inorganic chemistry*, 2012, **51**, 215.
18. Y. M. You and S. Y. Park, *Journal of the American Chemical Society*, 2005, **127**, 12438.
19. E. Baranoff, B. F. E. Curchod, F. Monti, F. Steimer, G. Accorsi, I. Tavernelli, U. Rothlisberger, R. Scopelliti, M. Grätzel and M. K. Nazeeruddin, *Inorganic Chemistry*, 2012, **51**, 799.
20. M. Muller, A. Devaux, C. H. Yang, L. De Cola and R. A. Fischer, *Photochem. Photobiol. Sci.*, 2010, **9**, 846.
21. M. L. Xu, G. B. Che, X. Y. Li and Q. Xiao, *Acta Crystallogr., Sect. E: Struct. Rep. Online*, 2009, **65**, M28.
22. B. D. Muegge and M. M. Richter, *Luminescence : the journal of biological and chemical luminescence*, 2005, **20**, 76.
23. B. Dandrade, S. Datta, S. Forrest, P. Djurovich, E. Polikarpov and M. Thompson, *Organic Electronics*, 2005, **6**, 11.
24. E. Orselli, G. S. Kottas, A. E. Konradsson, P. Coppo, R. Fröhlich, L. De Cola, A. van Dijken, M. Buchel and H. Börner, *Inorganic Chemistry*, 2007, **46**, 11082.
25. J. Frey, B. F. E. Curchod, R. Scopelliti, I. Tavernelli, U. Rothlisberger, M. K. Nazeeruddin and E. Baranoff, *Dalton Transactions*, 2014, **43**, 5667.
26. Y. Y. Zhou, W. F. Li, Y. Liu, L. Q. Zeng, W. M. Su and M. Zhou, *Dalton Transactions*, 2012, **41**, 9373.
27. J. Pommerehne, H. Vestweber, W. Guss, R. F. Mahrt, H. Bassler, M. Porsch and J. Daub, *Adv. Mater.*, 1995, **7**, 551.
28. C. M. Cardona, W. Li, A. E. Kaifer, D. Stockdale and G. C. Bazan, *Adv. Mater.*, 2011, **23**, 2367.
29. V. I. Adamovich, S. R. Cordero, P. I. Djurovich, A. Tamayo, M. E. Thompson, B. W. D'Andrade and S. R. Forrest, *Organic Electronics*, 2003, **4**, 77.
30. T. Motoyama, Y. Agata and J. Kido, *Journal of Photopolymer Science and Technology*, 2006, **19**, 663.
31. H. Y. Shi, L. L. Deng, S. F. Chen, Y. Xu, X. F. Zhao, F. Cheng and W. Huang, *Aip Advances*, 2014, **4**.
32. S. P. Huang, T. H. Jen, Y. C. Chen, A. E. Hsiao, S. H. Yin, H. Y. Chen and S. A. Chen, *Journal of the American Chemical Society*, 2008, **130**, 4699.
33. C. H. Hsiao, S. W. Liu, C. T. Chen and J. H. Lee, *Organic Electronics*, 2010, **11**, 1500.
34. Y. B. Zhao, L. P. Zhu, J. S. Chen and D. G. Ma, *Organic Electronics*, 2012, **13**, 1340.
35. S. Y. Lee, Y. H. Kim, W. Song, M. Mei, R. Wood and W. Y. Kim, *Japanese Journal of Applied Physics*, 2011, **50**.
36. A. F. Rausch, M. E. Thompson and H. Yersin, *Inorganic Chemistry*, 2009, **48**, 1928.
37. A. F. Rausch, M. E. Thompson and H. Yersin, *Journal of Physical Chemistry A*, 2009, **113**, 5927.
38. C. Adachi, R. C. Kwong, P. Djurovich, V. Adamovich, M. A. Baldo, M. E. Thompson and S. R. Forrest, *Applied Physics Letters*, 2001, **79**, 2082.
39. V. N. Kozhevnikov, Y. H. Zheng, M. Clough, H. A. Al-Attar, G. C. Griffiths, K. Abdullah, S. Raisys, V. Jankus, M. R. Bryce and A. P. Monkman, *Chemistry of Materials*, 2013, **25**, 2352.
40. S. L. Tao, S. L. Lai, C. A. Wu, T. W. Ng, M. Y. Chan, W. M. Zhao and X. H. Zhang, *Organic Electronics*, 2011, **12**, 2061.
41. T. Tsuboi, H. Murayama, S.-J. Yeh, M.-F. Wu and C.-T. Chen, *Optical Materials*, 2008, **31**, 366.

Dalton Transactions Accepted Manuscript

42. A. Endo, K. Suzuki, T. Yoshihara, S. Tobita, M. Yahiro and C. Adachi, *Chemical Physics Letters*, 2008, **460**, 155.
43. T. Tsuboi, H. Murayama, S.-J. Yeh and C.-T. Chen, *Optical Materials*, 2007, **29**, 1299.
44. J. Li, P. I. Djurovich, B. D. Alleyne, M. Yousufuddin, N. N. Ho, J. C. Thomas, J. C. Peters, R. Bau and M. E. Thompson, *Inorganic Chemistry*, 2005, **44**, 1713.
45. S. Kodate and I. Suzuka, *Japanese Journal of Applied Physics*, 2006, **45**, 574.
46. I. Tanaka, Y. Tabata and S. Tokito, *Chemical Physics Letters*, 2004, **400**, 86.
47. Y. Kawamura, K. Goushi, J. Brooks, J. J. Brown, H. Sasabe and C. Adachi, *Applied Physics Letters*, 2005, **86**, 071104.
48. Y. Kawamura, J. Brooks, J. Brown, H. Sasabe and C. Adachi, *Physical Review Letters*, 2006, **96**.
49. N. Matsusue, S. Ikame, Y. Suzuki and H. Naito, *Journal of Applied Physics*, 2005, **97**, 123512.
50. P. Hohenberg and W. Kohn, *Phys. Rev. B*, 1964, **136**, B864.
51. W. Kohn and L. J. Sham, *Phys. Rev.*, 1965, **140**, 1133.
52. E. Runge and E. K. U. Gross, *Phys. Rev. Lett.*, 1984, **52**, 997.
53. M. E. Casida, in *Recent Advances in Density Functional Methods*, ed. D. P. Chong, Singapore, World Scientific, 1995, p. 155.
54. M. Petersilka, U. J. Gossmann and E. K. U. Gross, *Phys. Rev. Lett.*, 1996, **76**, 1212.
55. C. A. Ullrich and Z. H. Yang, *Brazilian Journal of Physics*, 2014, **44**, 154.
56. P. J. Hay, *J. Phys. Chem. A*, 2002, **106**, 1634.
57. F. De Angelis, F. Santoro, M. K. Nazeruddin and V. Barone, *Journal of Physical Chemistry B*, 2008, **112**, 13181.
58. F. De Angelis, L. Belpassi and S. Fantacci, *J. Mol. Struc. (Theochem)*, 2009, **914**, 74
59. N. G. Park, G. C. Choi, Y. H. Lee and Y. S. Kim, *Curr. Appl. Phys.*, 2006, **6**, 620.
60. A. D. Becke, *J. Chem. Phys.*, 1993, **98**, 5648.
61. C. Lee, W. Yang and R. G. Parr, *Phys. Rev. B*, 1988, **37**, 785.
62. X. Gu, T. Fei, H. Y. Zhang, H. Xu, B. Yang, Y. G. Ma and X. D. Liu, *Journal of Physical Chemistry A*, 2008, **112**, 8387.
63. C. Adamo and V. Barone, *J. Chem. Phys.*, 1999, **110**, 6158.
64. S. Koseki, N.-o. Kamata, T. Asada, S. Yagi, H. Nakazumi and T. Matsushita, *J. Phys. Chem. C*, 2013, **117**, 5314.
65. H.-R. Tsai, K.-Y. Lu, S.-H. Lai, C.-H. Fan, C.-H. Cheng and I. C. Chen, *J. Phys. Chem. C*, 2011, **115**, 17163.
66. Y. Zhao and D. G. Truhlar, *Theor. Chem. Acc.*, 2008, **120**, 215.
67. Y. Zhao, N. E. Schultz and D. G. Truhlar, *Journal of Chemical Theory and Computation*, 2006, **2**, 364.
68. H. F. Li, P. Winget, C. Risko, J. S. Sears and J. L. Bredas, *Physical Chemistry Chemical Physics*, 2013, **15**, 6293.
69. E. J. Baerends, O. V. Gritsenko and R. van Meer, *Physical Chemistry Chemical Physics*, 2013, **15**, 16408.
70. E. J. Baerends and O. V. Gritsenko, *Journal of Physical Chemistry A*, 1997, **101**, 5383.
71. B. Yang, M. Zhang, H. Zhang and J.-Z. Sun, *Journal of Luminescence*, 2011, **131**, 1158.
72. B. Himmetoglu, A. Marchenko, I. Dabo and M. Cococcioni, *J. Chem. Phys.*, 2012, **137**, 154309.
73. J. J. Brooks, R. C. Kwong, Y. J. Tung, M. S. Weaver, B. W. D'andrade, V. Adamovich, M. E. Thompson, S. R. Forrest and J. J. Brown, *P Soc Photo-Opt Ins*, 2004, **5519**, 35.
74. H. Iikura, T. Tsuneda, T. Yanai and K. Hirao, *J. Chem. Phys.*, 2001, **115**, 3540.
75. E. Baranoff, S. Fantacci, F. De Angelis, X. X. Zhang, R. Scopelliti, M. Gratzel and M. K. Nazeeruddin, *Inorganic chemistry*, 2011, **50**, 451.
76. A. R. G. Smith, P. L. Burn and B. J. Powell, *ChemPhysChem*, 2011, **12**, 2428.

Dalton Transactions Accepted Manuscript

77. E. Jansson, B. Minaev, S. Schrader and H. Agren, *Chemical physics*, 2007, **333**, 157.
78. X. Li, B. Minaev, H. Agren and H. Tian, *European Journal of Inorganic Chemistry*, 2011, 2517.
79. T. Matsushita, T. Asada and S. Koseki, *J. Phys. Chem. C*, 2007, **111**, 6897.
80. B. Minaev, H. Agren and F. De Angelis, *Chemical physics*, 2009, **358**, 245.
81. K. Mori, T. Goumans, E. van Lenthe and F. Wang, *Physical Chemistry Chemical Physics*, 2014.
82. A. R. G. Smith, M. J. Riley, P. L. Burn, I. R. Gentle, S. C. Lo and B. J. Powell, *Inorganic chemistry*, 2012, **51**, 2821.
83. J. M. Younker and K. D. Dobbs, *Journal of Physical Chemistry C*, 2013, **117**, 25714.
84. B. Minaev, G. Baryshnikov and H. Agren, *Physical Chemistry Chemical Physics*, 2014, **16**, 1719.
85. I. Tanaka, M. Suzuki and S. Tokito, *Japanese Journal of Applied Physics*, 2003, **42**, 2737.
86. Y. Kawamura, S. Yanagida and S. R. Forrest, *Journal of Applied Physics*, 2002, **92**, 87.
87. R. J. Holmes, S. R. Forrest, Y. J. Tung, R. C. Kwong, J. J. Brown, S. Garon and M. E. Thompson, *Applied Physics Letters*, 2003, **82**, 2422.
88. S. Tokito, T. Iijima, Y. Suzuri, H. Kita, T. Tsuzuki and F. Sato, *Applied Physics Letters*, 2003, **83**, 569.
89. M. H. Tsai, H. W. Lin, H. C. Su, T. H. Ke, C. c. Wu, F. C. Fang, Y. L. Liao, K. T. Wong and C. I. Wu, *Adv. Mater.*, 2006, **18**, 1216.
90. D. Tanaka, T. Takeda, T. Chiba, S. Watanabe and J. Kido, *Chemistry Letters*, 2007, **36**, 262.
91. D. Tanaka, Y. Agata, T. Takeda, S. Watanabe and J. Kido, *Japanese Journal of Applied Physics*, 2007, **46**, L117.
92. N. Chopra, J. Lee, Y. Zheng, S.-H. Eom, J. Xue and F. So, *Applied Physics Letters*, 2008, **93**, 143307.
93. C. W. Lee and J. Y. Lee, *Adv. Mater.*, 2013, **25**, 5450.
94. M. K. Mathai, V.-E. Choong, S. A. Choulis, B. Krummacher and F. So, *Applied Physics Letters*, 2006, **88**, 243512.
95. S. Y. Shao, J. Q. Ding, T. L. Ye, Z. Y. Xie, L. X. Wang, X. B. Jing and F. S. Wang, *Advanced Materials*, 2011, **23**, 3570.
96. D. Sun, X. Zhou, H. F. Li, X. Sun, Y. Zheng, Z. Ren, D. Ma, M. R. Bryce and S. Yan, *J. Mater. Chem. C*, 2014, **2**, 8277.
97. C. L. Mulder, K. Celebi, K. M. Milaninia and M. A. Baldo, *Applied Physics Letters*, 2007, **90**, 211109.
98. J. Lee, J.-I. Lee, J. Y. Lee and H. Y. Chu, *Organic Electronics*, 2009, **10**, 1529.
99. M.-T. Lee, J.-S. Lin, M.-T. Chu and M.-R. Tseng, *Applied Physics Letters*, 2009, **94**, 083506.
100. H. S. Fu, Y. M. Cheng, P. T. Chou and Y. Chi, *Materials Today*, 2011, **14**, 472.
101. T. Sajoto, P. I. Djurovich, A. B. Tamayo, J. Oxgaard, W. A. Goddard and M. E. Thompson, *Journal of the American Chemical Society*, 2009, **131**, 9813.
102. A. Batagin-Neto, A. P. Assis, J. F. Lima, C. J. Magon, L. Yan, M. Shao, B. Hu and C. F. Graeff, *J. Phys. Chem. A*, 2014.
103. V. Sivasubramaniam, F. Brodkorb, S. Hanning, H. P. Loebl, V. van Elsbergen, H. Boerner, U. Scherf and M. Kreyenschmidt, *Journal of Fluorine Chemistry*, 2009, **130**, 640.
104. E. Baranoff, S. Suarez, P. Bugnon, C. Barolo, R. Buscaino, R. Scopelliti, L. Zuppiroli, M. Graetzel and M. K. Nazeeruddin, *Inorganic chemistry*, 2008, **47**, 6575.
105. Y. Zheng, A. S. Batsanov, R. M. Edkins, A. Beeby and M. R. Bryce, *Inorganic chemistry*, 2012, **51**, 290.
106. V. Sivasubramaniam, F. Brodkorb, S. Hanning, O. Buttler, H. P. Loebl, V. van Elsbergen, H. Boerner, U. Scherf and M. Kreyenschmidt, *Solid State Sciences*, 2009, **11**, 1933.

Dalton Transactions Accepted Manuscript

Dalton Transactions Accepted Manuscript